STAR: Science & Technology of Archaeological Research

ISSN: (Print) 2054-8923 (Online) Journal homepage: https://www.tandfonline.com/loi/ysta20

A methodology for qualitative archaeometallurgical fieldwork using a handheld X-ray fluorescence spectrometer

R.B. Scott, K. Eekelers, L. Fredericks & P. Degryse

To cite this article: R.B. Scott, K. Eekelers, L. Fredericks & P. Degryse (2015) A methodology for qualitative archaeometallurgical fieldwork using a handheld X-ray fluorescence spectrometer, STAR: Science & Technology of Archaeological Research, 1:2, 70-80, DOI: 10.1080/20548923.2016.1183941

To link to this article: https://doi.org/10.1080/20548923.2016.1183941

Published online: 23 May 2016.

Science and Technology of Archaeological Research

Research Article

A methodology for qualitative archaeometallurgical fieldwork using a handheld X-ray fluorescence spectrometer

R.B. Scott*, K. Eekelers, L. Fredericks, and P. Degryse

Division Geology, KU Leuven, Celestijnenlaan 200E, 3001 Leuven, Belgium

Abstract Recent work aimed at provenancing metal slag from Sagalassos, south-west Turkey, as part of a study investigating the Roman iron industry in the area. Although previously samples of the slag material had been exported from the country for the purposes of analysis, a method of analysing the materials in-situ was required. It was decided that the best technique for achieving 'in-the-field' results would be handheld X-ray fluorescence spectrometry (HH-XRF). A series of laboratory based tests were first performed in order to determine the ideal working parameters for the HH-XRF and the best method for preparing the samples. The results indicated that different slag (i.e. Ti-rich/poor) could clearly be distinguished amongst the powdered samples.

A total of 45 metal slag were analysed in the field in order to see whether the slag could be qualitatively characterised based on provenance. The results of the field study indicated two principle groups (a high Ti – Zr group and a low Ti – Zr group). The Ca and Mn contents also split the data into two groups but these were not consistent with the previous Ti – Zr groups. These differences could be related to the choice of ores and fluxes used for iron production.

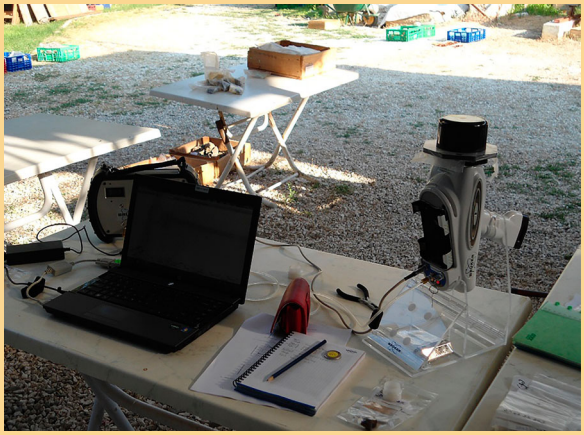

Keywords HH-XRF; Iron slag; Field laboratory; Roman; Sagalassos

Received 17 June 2015; **accepted** 29 March 2016

Introduction

Portable X-ray Fluorescence Spectrometry (pXRF) is very attractive for use in archaeological projects. The instrumentation can be taken to the objects/materials rather than a need for samples to be taken to the laboratory for analysis. In addition pXRF is a non-destructive technique, meaning that valuable and/or sensitive archaeological material can be analysed. Portable XRF technology is nothing new, and has been used in a variety of industries including metals, mining and geosciences (Helmig, Jackwerth, and Hauptmann 1989; Speakman et al. 2011; Goren, Mommsen, and Klinger 2011). Since Helmig, Jackwerth, and Hauptmann (1989) wrote their paper, technology has improved and miniaturised, resulting in the development of handheld devices (HH-XRF). In

*Corresponding author. email: becki.scott@ees.kuleuven.be

this context, pXRF refers to any XRF device which is portable and can be taken to a museum or field laboratory. HH-XRF refers specifically to the range of handheld devices. In the last 25 years, the use of p- and HH-XRF for a wide variety of archaeological applications has seen a dramatic increase (Mantler and Schreiner 2000; Carter and Shackley 2007; Shackley 2011a; Shackley 2012; Speakman and Shackley 2013; Hunt and Speakman 2015; Schreiner et al. 2004; A. N. Shugar and Mass 2012; Craig et al. 2007; Goren, Mommsen, and Klinger 2011; Speakman et al. 2011; Nakai et al. 2005).

Generally, when a pXRF is taken to the field for analytical reasons, it is either for screening materials prior to further analysis, or because an on-site assemblage contains a large volume of material and a rapid collection of analytical data is required (Helmig, Jackwerth, and Hauptmann 1989; Shackley 2011b; Liritzis and Zacharias 2011). The continued improvement and miniaturisation of the instrumentation has made pXRF, in particular HH-XRF, spectrometers affordable to a wide variety of archaeological, museum and heritage workers (Forster et al. 2011; Nicholas and Manti 2014; A. N. Shugar and Mass 2012). However, these machines have usually been designed with a specific industry in mind and although they can be applied to archaeological material, they are rarely made specifically for this purpose. Current HH-XRF spectrometers are often marketed as 'point and shoot' devices, meaning that the user can analyse and quantify the chemical composition of a material using the factory settings (Hunt and Speakman 2015; Shackley 2012). While this 'black box' approach has received much debate in the literature (Speakman and Shackley 2013; Hunt and Speakman 2015; Speakman et al. 2011; Shackley 2010; Jia et al. 2010; Sheppard et al. 2011; Nazaroff, Prufer, and Drake 2010; Shackley 2011b; Frahm 2013), and studies have been undertaken which review the application of HH-XRF to homogeneous material (e.g. Nazaroff, Prufer, and Drake 2010; Goren, Mommsen, and Klinger 2011), the studies on the application of this technology to heterogeneous material (e.g. Nicholas and Manti 2014; Hunt and Speakman 2015; Forster et al. 2011) are a relatively recent development.

Since one of the primary uses for pXRF was in the mining industry, the use of handheld spectrometers to analyse the composition of metal ores is relatively established (Simandl et al. 2014). However, Helmig, Jackwerth, and Hauptmann (1989) were the first to use a pXRF spectrometer to analyse the composition of metal slag. Yet, little, if any, further work on the use of pXRF (or specifically HH-XRF) for the analysis of metal slag has been published. While the advancement and further development of the instrumentation is fairly obvious; has the methodology for the analysis of archaeological material in the field, particularly metal slag, also advanced? This paper explores the best method for analysing Fe-rich slag in the field and compares the outcomes with the method originally outlined by Helmig, Jackwerth, and Hauptmann (1989).

Background

Sagalassos, Turkey, is the site of a Hellenistic to Byzantine city and has been the subject of ongoing archaeological excavation and research since 1986. A current research project is investigating the Roman iron working practices in and around the Sagalassos region, in an attempt to reconstruct the economic networks of the city and its territories (Degryse, Muchez, Naud, et al. 2003; Degryse, Muchez, Six, et al. 2003; Waelkens et al. 1999; Degryse et al. 2007; Degryse, Poblome, et al. 2003). Iron slag has frequently been found during excavation in the city, dating stratigraphically from the 1st to 7th centuries AD, indicating the presence of iron working at the site (Degryse, Muchez, Six, et al. 2003; Kucha et al. 1995; Degryse et al. 2007). Iron slag have also been identified in the surrounding area, up to 25 km south-east of the city (Figure 1 – map of slag find locations). These latter finds have been dated to the 6th – 7th centuries (Degryse et al. 2007). An analysis of the chemical composition of the slag allows inferences to be made about the original ore source. This in turn allows a targeted exploration of the area around Sagalassos to determine whether the ore used in the iron production was of a local origin. Previous research had identified two main chemical groups. The samples from Sagalassos have the signature of a typical Roman slag (high FeO and SiO_2 contents and moderate to low contents of other elements) (Degryse et al. 2007). The samples from the wider area appeared to have elevated TiO_2, V_2O_5, CaO, MgO and Zr, associated with a placer deposit in the Bey Dağlari area (Degryse, Muchez, Six, et al. 2003; Degryse et al. 2007).

Previously, samples of archaeological iron slag and associated ore had been exported to KU Leuven, Belgium for destructive analysis. However, the majority of the iron slag samples remained in Turkey. Although this collection remains available for study in Turkey, due to a change in legislation, it was not possible to export further samples for analysis. Therefore a method of analysing the material in the field was required. Since there was no prior established procedure for the analysis of iron slag using HH-XRF, the 2013 field campaign offered the perfect opportunity to test the method proposed by Helmig, Jackwerth, and Hauptmann (1989). Initially, laboratory tests were carried out to determine the ideal HH-XRF parameters for the analysis of iron slag, the best method of sample preparation and the validity of the subsequent qualitative data. The optimised conditions were then used in the field to gather data on the existent collection of iron slag samples in the Sagalassos excavation depot.

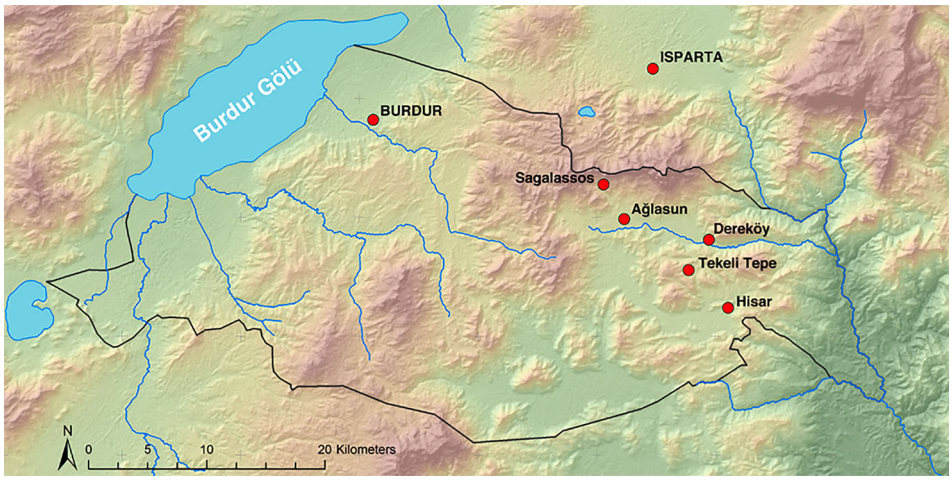

Figure 1 Map of the Sagalassos region of Turkey, indicating the find locations of the slag.

Method

A Bruker Tracer III SD was used at three different measurement settings; 40 kV, 10.9 μA to determine the full range of elements present in the samples; 15 kV, 5 μA to determine the light elements in the samples, and 9 kV, 20 μA to specifically interrogate light elements of particular interest (Al, Si, P, K, Ca, Ti, V, Mn, Fe, Zr). A vacuum was used in all cases in order to attain the best measurements possible on the light elements. All measurements were made for 90 seconds. The spectra were collected using the Bruker S1PXRF program and were subsequently analysed with the Bruker ARTAX software.

In the laboratory, four samples of iron slag were each prepared in four different ways and measured, in order to determine the most reliable preparation method. Initially the slag were cut in half and measurements made on the 'flat' internal surface, and the unprepared external surface. Several small cubes, c. 1 cm^3, were cut from each of the slag, this allowed the internal structure of the slag to be maintained (as with the previous preparation method) but more faces could be analysed. Lastly, the samples were powdered; the oxidation of the outer layers was first removed with a diamond saw, then the samples were dried for 24 hours at 60 °C. Next the samples were crushed with a hammer and then ground with a mortar and pestle. Finally the samples were placed in a ball mill for 10 minutes to further grind the samples to a fine powder.

Finally, 40 samples of powdered slag were measured for a further 300 seconds each, this was primarily with the aim of creating a quantification calibration at a later date, but also to enable a thorough qualitative comparison of the data, with particular focus on the trace elements.

The first challenge in the field was 'how' to powder the samples. Although the count rate increases as the grain size of the samples decreases, sifting of the samples is not necessary in the field, as long as the ground samples are approximately uniform in size (Helmig, Jackwerth, and Hauptmann 1989). In Sagalassos, the outer surfaces of the slag were first removed (as far as possible) by placing them on a metal plate and striking them with a hammer. The slag were then powdered by wrapping the samples in plastic and then placing inside plastic bags, and again striking them with a geology hammer. The collected powder was sieved through a fine mesh to ensure as homogeneous a grain size as possible. The samples were then placed into sample cups and measured for 60 seconds each.

Results

In terms of the instrument settings used, 40 kV, 10.9 μA provided a general overview of the whole range of elements present in the iron slag. The lower energy settings of 15 kV, 5 μA and 9 kV, 20 μA provided much better counts on the light elements. However, since the K lines of all the elements of interest (Al, Si, P, K, Ca, Ti, V, Mn, Fe and Zr L lines) were present in the spectra at 9 kV, it was decided that in the field the 15 kV setting would not be necessary. The Zr L lines are present in the spectra at 9 kV and these can also be interrogated in qualitative analyses.

Table 1 shows the standard deviations for repeat measurements of the four samples prepared in four different ways, based on the measurements made at 9 kV, 20 μA. Both one-way and two-way ANOVA tests indicated that there was a statistically significant difference between the measured HH-XRF counts for each element using different sample preparation methods. However, these tests only indicate that there is a statistically significant difference, not where that significant difference occurs. In other words, a further statistical test was needed to identify which type(s) of sample preparation made the biggest difference to the measured counts. A Tukey HSD test was performed on the data because this, while not as robust as the ANOVA tests on its own, when used in conjunction will indicate which method of preparation resulted in a statistically

Table 1 Net peak area counts of repeat measurements of four samples prepared in different ways, average variances of the data for each sample type, and total SD for each sample type.

Sample	Type	Al	Ca	Cr	Fe	K	Mn	Si	Ti
NK064	powder	1	26819	578	156116	1122	2724	3152	713
NK064	powder	28	16951	540	158959	681	2766	2098	805
NK064	powder	1	10153	603	165735	377	3326	1619	668
NK064	powder	1	28471	405	135645	1455	1735	3441	796
NK064	powder	138	30038	611	128745	3565	1475	4073	990
FCG27	powder	119	11283	1445	101071	1415	3861	2880	29701
FCG27	powder	90	11513	1350	100023	1435	3998	2869	27597
FCG27	powder	74	11651	1308	101545	1461	4018	2895	28518
FCG27	powder	138	12058	970	101877	1569	3853	3254	21021
FCG27	powder	154	13464	1164	106198	1836	4270	4739	24208
NK138	powder	63	30771	641	148253	684	2071	2900	688
NK138	powder	104	30593	367	131904	242	1499	2246	788
NK138	powder	1	30189	430	135927	1012	1529	2707	526
NK138	powder	6	15409	435	151017	245	1781	2702	694
NK138	powder	4	22950	588	139790	461	1694	2406	620
NK018	powder	198	8132	568	112599	885	5132	1966	30737
NK018	powder	56	11084	746	112965	954	3595	2033	12909
NK018	powder	82	12280	778	119677	1200	3886	2857	13441
NK018	powder	110	9126	605	120303	837	5245	2086	28563
NK018	powder	135	7671	473	109740	752	4841	2203	26094
NK064	solid ex	149	11268	1399	314531	2566	3674	2939	3599
NK064	solid ex	96	16028	1062	228005	4453	5773	3255	4150
NK064	solid ex	3	24375	1614	376581	3723	4776	3951	4301
FCG27	solid ex	150	21200	3288	268021	3230	9336	3460	46549
FCG27	solid ex	190	17513	3373	281737	1595	11111	3729	67391
FCG27	solid ex	95	21320	2333	248744	1590	11063	3001	55720
NK138	solid ex	1	40994	1031	160435	4597	4369	3333	3942
NK138	solid ex	131	72872	1145	147060	8375	4559	6715	5871
NK138	solid ex	66	102193	1333	187461	7212	4525	6049	4939
NK018	solid ex	161	73642	1841	236514	4735	7625	6955	19883
NK018	solid ex	50	73479	1992	178122	1291	8446	2293	67750
NK018	solid ex	-8	119894	2012	196555	5761	7498	6809	17240
NK064	solid in	60	28745	1277	381382	577	4712	2606	1818
NK064	solid in	47	8202	1077	305015	570	5302	2069	1908
NK064	solid in	1	25927	1640	361259	1292	5059	3244	1174
FCG27	solid in	44	36098	1516	268406	2653	13964	3742	70910
FCG27	solid in	1	27971	1555	256798	2620	12559	2919	87254
FCG27	solid in	127	39099	1844	282936	3195	14773	4118	77660
NK138	solid in	104	35242	1103	306854	1896	5436	3010	2035
NK138	solid in	53	4818	1949	372487	5	3978	2251	1443
NK138	solid in	1	5316	2109	441356	36	5356	3164	1225
NK018	solid in	32	10628	863	296627	390	10946	2034	18698
NK018	solid in	1	13931	1019	346889	465	16200	2545	19825
NK018	solid in	60	19331	1026	295956	659	11243	2373	32314
NK064	cube	1	50615	993	115233	1348	2094	5189	656
NK064	cube	132	31734	1363	129473	4000	1821	6239	1196
NK064	cube	1	51027	1126	116534	1627	2114	5083	750
NK064	cube	162	35764	1226	129529	4961	2121	6639	999
NK064	cube	95	34308	1148	126423	4485	2003	5739	1336
NK064	cube	246	7326	1217	121757	1766	2097	4731	1759
NK064	cube	94	31202	1271	139134	3983	2166	5674	1136
NK064	cube	487	11239	1046	113216	1895	2046	5596	1518
NK064	cube	66	29648	1062	120022	3395	1964	5086	1147
NK064	cube	1	10727	1616	176079	362	4155	2235	801
NK064	cube	7	9472	1629	165959	309	2636	1934	917
NK064	cube	1	3524	1402	169638	464	3464	1710	1140
NK064	cube	33	19985	1328	153438	437	2854	2087	753
NK064	cube	6	18761	1324	154004	419	2915	2034	720
NK064	cube	1	20546	1569	154580	698	2942	2354	814
NK064	cube	46	26219	1457	150904	971	2935	3129	1151
NK064	cube	30	16983	1231	147063	1033	4842	2515	759
NK064	cube	1	13931	1554	163593	391	3691	2281	1390
NK064	cube	46	22233	1554	153227	957	2681	2454	1302
NK064	cube	144	15177	1401	156355	1521	2758	3710	1149
NK064	cube	420	9209	1051	103723	2071	1841	5885	2051
FCG27	cube	84	10698	1885	108246	1116	4412	2744	28830
FCG27	cube	84	12795	1624	111154	1406	4614	3751	30280
FCG27	cube	585	8175	2011	105180	1201	4451	5512	26851

(*Continued*)

Table 1 Continued.

Sample	Type	Al	Ca	Cr	Fe	K	Mn	Si	Ti
FCG27	cube	186	14541	1401	117179	1660	5056	4499	26780
FCG27	cube	223	14981	1625	126005	1875	5261	4298	26899
FCG27	cube	957	7596	1191	85641	2500	4023	7611	14300
FCG27	cube	206	9821	1562	101966	1038	4205	2363	23437
FCG27	cube	94	11127	1707	119121	1354	5072	3964	25345
FCG27	cube	595	10476	1823	101133	1967	4062	6714	12112
FCG27	cube	142	12008	2032	112448	1447	4773	3499	29345
FCG27	cube	124	11301	1804	108293	1372	4705	3227	28773
FCG27	cube	100	10500	1400	96802	1295	4067	2785	24942
FCG27	cube	167	10411	1724	110384	1207	4486	2869	28514
FCG27	cube	152	9683	1694	102650	1132	3950	2879	25344
FCG27	cube	259	12409	1782	112585	1320	4663	3494	29452
FCG27	cube	158	11827	2168	117231	1380	4634	3013	31865
FCG27	cube	276	10757	1342	116814	1637	4635	4216	24545
FCG27	cube	300	11734	2083	117226	1416	4880	3326	31975
NK138	cube	0	26619	1154	117413	662	2261	1955	372
NK138	cube	1	32537	1256	131816	978	2570	2439	636
NK138	cube	189	39001	771	109037	1349	1897	3790	548
NK138	cube	101	21693	1663	156962	413	2796	1602	997
NK138	cube	1	24213	1679	166250	697	3067	2285	770
NK138	cube	296	28488	1016	84404	2193	2733	4727	1628
NK138	cube	1	71366	805	91411	397	1589	2263	529
NK138	cube	40	62753	870	102040	409	1756	3256	616
NK138	cube	321	36839	687	36349	3484	2068	7247	1776
NK138	cube	1	34022	1777	147191	662	3002	1846	784
NK138	cube	1	28839	1482	145847	434	2509	1589	941
NK138	cube	108	23852	900	70210	2347	1843	4280	1456
NK138	cube	1	16578	1129	137683	276	2342	3091	882
NK138	cube	1	3557	1269	152575	175	2713	2900	638
NK138	cube	212	33359	699	68389	1983	2172	5034	1391
NK018	cube	33	11515	1450	140644	1060	4750	2514	14652
NK018	cube	149	11506	1335	129776	1240	4648	3248	13503
NK018	cube	377	81488	1023	66871	2311	2551	8032	6005
NK018	cube	1	10803	1240	128543	786	4595	1498	10356
NK018	cube	217	14472	1680	126276	1186	4840	3217	12174
NK018	cube	356	42454	1226	102605	1603	3524	5914	7683
NK018	cube	1	8945	1149	131817	591	4993	2563	12143
NK018	cube	111	9350	1639	145673	1373	4874	3773	14732
NK018	cube	365	15880	1587	92488	1345	3685	7162	8460
NK018	cube	131	10891	1696	138949	1320	4693	3005	14061
NK018	cube	125	11913	1721	132036	1299	4469	3259	13584
NK018	cube	119	12866	1400	131246	1163	4841	2731	13882
NK018	cube	48	7497	843	135110	658	5458	1794	21782
NK018	cube	147	6780	1123	152093	815	6019	1677	24453
NK018	cube	34	4355	731	111553	358	3795	741	13355
NK018	cube	96	6509	981	121742	429	4485	1045	14524
NK018	cube	85	9883	933	99175	391	3584	1083	9599
NK018	cube	82	7826	822	108123	593	4537	1583	25258
NK018	cube	110	10695	1161	128533	913	5036	1738	20706
NK018	cube	137	7602	1112	131409	717	4054	1913	20603
NK018	cube	87	12035	1127	126460	1002	4794	1823	19550
NK018	cube	166	8163	1137	140036	955	5872	2194	14250
NK018	cube	151	6416	943	124237	541	5081	1464	19401
NK018	cube	24	6432	966	129037	642	4394	1237	14581

	Average Variance	Al	Ca	Cr	Fe	K	Mn	Si	Ti
	powder	2429	30983171	17756	86920549	436564	311244	462900	21370854
	solid ex	4834	425295704	110722	1789487805	2756415	600006	2659558	229608607
	solid in	2147	120010974	103570	1778817091	367088	2681395	257139	31224586
	cube	23907	179449194	84072	592428536	879477	400305	2734325	13589563

	SD	Al	Ca	Cr	Fe	K	Mn	Si	Ti
	powder	49	5566	133	9323	661	558	680	4623
	solid ex	70	20623	333	42302	1660	775	1631	15153
	solid in	46	10955	322	42176	606	1637	507	5588
	cube	155	13396	290	24340	938	633	1654	3686

Table 2 Results of the Tukey HSD test, where the Q-critical is 3.6863. If the Q value in the table is above this number then a statistically significant difference exists between the samples, i.e. the p<0.05. P is powder; SE is the external surface of the slag; SI is the internal surface; C is cube. Grey cells indicate a statistically significant difference exists between the preparation methods.

		Al						Ti			
		P	SE	SI	C			P	SE	SI	C
Al	P		0.4308	0.8767	2.7962	Ti	P		2.9618	3.2540	0.4783
	SE	0.4308		1.1695	1.7528		SE	2.9618		0.2614	3.8743
	SI	0.8767	1.1695		3.2925		SI	3.2540	0.2614		4.2184
	C	2.7962	1.7528	2.7962			C	0.4783	3.8743	4.2184	
		Si						Cr			
		P	SE	SI	C			P	SE	SI	C
Si	P		4.0735	0.2097	2.4262	Cr	P		10.5915	6.3696	8.2806
	SE	4.0735		3.4559	2.8358		SE	10.5915		3.7761	5.7791
	SI	0.2097	3.4559		1.7141		SI	6.3696	3.7761		0.8076
	C	2.4262	2.8358	1.7141			C	8.2806	5.7791	0.8076	
		K						Mn			
		P	SE	SI	C			P	SE	SI	C
K	P		10.1740	0.2969	1.0590	Mn	P		7.3904	11.8093	1.3360
	SE	10.1740		8.8343	11.1246		SE	7.3904		3.9524	7.6228
	SI	0.2969	8.8343		0.5063		SI	11.8093	3.9524		12.8264
	C	1.0590	11.1246	0.5063			C	1.3360	7.6228	12.8264	
		Ca						Fe			
		P	SE	SI	C			P	SE	SI	C
Ca	P		7.0521	0.8245	0.5061	Fe	P		12.1008	22.2602	0.5767
	SE	7.0521		5.5702	7.8952		SE	12.1008		9.0869	14.7157
	SI	0.8245	5.5702		0.5618		SI	22.2602	9.0869		26.6791
	C	0.5061	7.8952	0.5618			C	0.5767	14.7157	26.6791	

significant difference. Table 2 gives the results of the Tukey HSD test, showing where a statistically significant difference occurred between the measured HH-XRF counts for the different sample preparation methods.

Figure 2 shows that at 40 kV, 10.9 μA the 40 samples of powdered slag (measured in the laboratory) could be separated into two groups, a high Ti – Zr group and a low Ti – Zr group. An independent, destructive, analysis by ICP-OES of the same samples showed the same high Ti – Zr and low Ti – Zr groups. The high Ti – Zr group consisted mainly of samples from Dereköy and Tekeli Tepe. The low Ti – Zr group was mostly samples from Sagalassos.

The laboratory data showed that the qualitative HH-XRF results were capable of distinguishing between different compositions of iron slag when the samples were powdered. Likewise, the analysis of 45 samples of iron slag powdered in the field (Figure 3) also showed the presence of a high Ti – Zr group and a low Ti – Zr group. However, in terms of the field data there was no obvious connection between

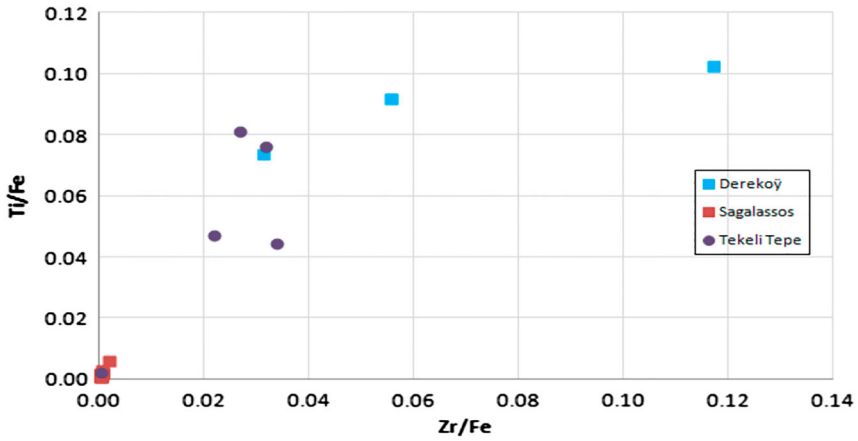

Figure 2 A biplot of Zr/Fe against Ti/Fe, measured using HH-XRF in the laboratory, indicating a high Ti-Zr group and a low Ti-Zr group.

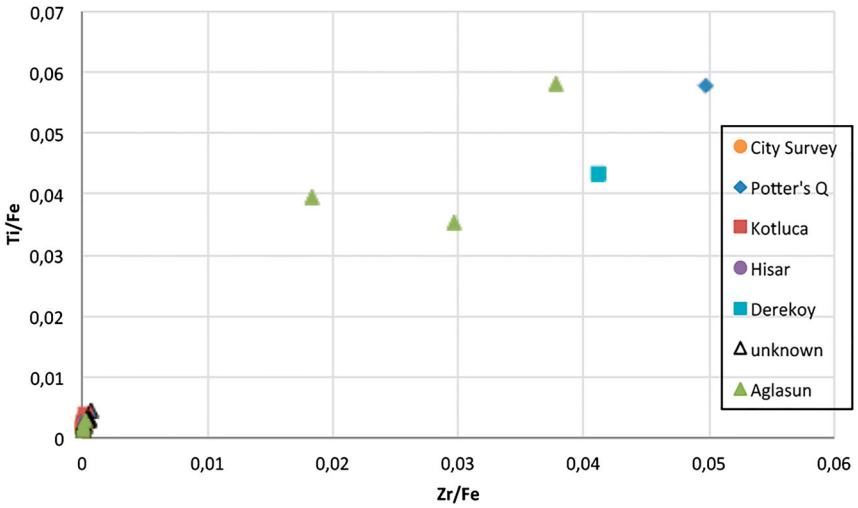

Figure 3 A biplot of Zr/Fe against Ti/Fe, measured using HH-XRF in the field, indicating a high Ti-Zr group and a low Ti-Zr group.

the find location of the slag and the resultant compositional group.

Discussion

Laboratory Analyses

The ANOVA tests revealed that the different methods of sample preparation resulted in a statistically significant difference between the measured HH-XRF counts for the elements. However, from the ANOVA tests it is only possible to say that there is a statistically significant difference between the highest and lowest mean values. A follow-up test was applied, a Tukey HSD test, this reveals between which specific sample preparation methods a statistically significant difference exists. From Table 2, it can be seen that there existed a significant difference for the fluorescence counts between the external surface of the solid slag and the other preparation methods for almost all the elements measured. This result is not surprising, since the external surface of the slag is uneven, will contain contamination from the burial environment, and in some cases the external surface had weathered. In addition, strongly oxidised surfaces can enhance the irregularity of the surface shapes (Mameli et al. 2014). The uneven surface will have increased the air gaps between the sample surface and the spectrometer and these air gaps will have increased the attenuation of the X-rays. While the measurements of the external surface of the slag may be consistent, they will ultimately misrepresent the bulk composition of the slag. Although an increased air gap would have reduced the detection of the light elements; it was noted in this case that the light elements in particular were elevated in the measurements of the external surface of the slag compared to the powders. This suggests that these slag had weathered resulting in a surface enrichment of light elements. Alternatively, more clay and soil from the burial environment may be adhering to the external surface of these slag. In terms of the mid-range elements (Ti, Cr, Mn, Fe) the measurements made on the internal surface of the slag also gave statistically significant differences to the HH-XRF counts, compared to the other preparation methods. Slag is a heterogeneous material, therefore, although multiple measurements were taken, these could represent completely different phases of the slag. Although the same can be said about the cubes, because these were also taken from the bulk of the slag, the cubes allowed measurements to be taken from more of the different phases. Although the cubes provided a flat surface and a measure of control in terms of analysing the bulk of the material without compromising the integrity of the structure of the slag, it was impossible to create cubes from the slag in the field. Powdering is therefore the optimum method of preparing the slag samples for field analysis. This is also reflected in the standard deviations (Table 1), where the powdering method does not always have the lowest standard deviation amongst the samples, but it does consistently have one of the lowest. It should however be remembered that the grain size of the powder may also affect the results (Hunt and Speakman 2015; Helmig, Jackwerth, and Hauptmann 1989).

After it was decided that powdering would be the optimum method of sample preparation, 40 samples of powdered slag were measured at both 40 kV, 10.9 µA and 9 kV, 20 µA. Figure 2 clearly shows that there are two groups amongst the slag, those which have high Ti and Zr and those with low Ti and Zr. The high Ti – Zr group is made up of samples from Dereköy and Tekeli Tepe, while the the low Ti – Zr group is mainly samples from the Sagalassos region. This fits well with previous research which had also identified two types of slag in the region (Degryse, Muchez, Six, et al. 2003; Degryse et al. 2007). Dereköy and Tekeli Tepe are both in the region of the Bey Dağlari massif which had previously been identified as the probable source of a high Fe, Ti, V group. This

latter group also had increased Zr levels, so it is probable that the slag found in this region originated from the spinel placer deposits at Bey Dağlari.

Field Analyses

Forty-five samples of iron slag were prepared in the field at Sagalassos for analysis. The first challenge was the method of sample preparation. Although the samples could be crushed and powdered with a hammer, this lacked the precision and control of the laboratory method of preparation. Likewise, although the best efforts were made to remove the outermost layers of the slag, prior to the bulk being powdered, there is a certain amount of the outer layers which will have contaminated the bulk of the sample. The method of powdering will not provide as fine a powder as had been created in the laboratory, and it is also very difficult to collect as much powder as possible, particularly with very hard samples. However, the results of the analysis also indicated the presence of two main groups, high Ti – Zr and low Ti – Zr samples. Helmig, Jackwerth, and Hauptmann (1989) noted that while different grain sizes did affect the measured results, as long as the samples were approximately uniformly prepared, the required accuracy and precision could still be achieved. In the case of the Sagalassos material, the same divisions could be observed in both the field and laboratory data.

The samples analysed in the field were labelled based on the find location of the slag. Figure 3 shows that, with the exception of one sample found in the Potter's Quarter area of the city, all of the Sagalassos material is part of the low Ti – Zr group. The samples from Ağlasun are split between the high Ti – Zr and the low Ti – Zr groups. This is explained by the fact that Ağlasun is not a smelting site, although smithing may have occurred there. It can be seen from Figure 1 that Ağlasun is situated between Sagalassos and Dereköy, it is therefore possible that material from both locations was used or transported through Ağlasun. Since Roman times slag have been used for road surfaces, but due to the low economic value of the material, it is not usually transported large distances (van Oss 2002). This was particularly the case from the late Roman period onwards, where a lot of iron work was devoted to satisfying the needs of the local area (Mameli et al. 2014; Buchwald and Wivel 1998). It is important, therefore, to remember that the deposition locations of all of the slag in this study are not necessarily the production locations. It is probable that the slag found in Sagalassos was produced somewhere in the city; it was often found in association with trade iron, iron artefacts and in the case of the early Roman period hematite ore. Likewise, the early Byzantine slag from Dereköy was found in association with furnace materials and was linked compositionally to local magnetite-titanite placer sands (Degryse et al. 2007). However, metallurgical waste and worked iron dating from the late Roman to early Byzantine period in Sagalassos proper has, as yet, no directly associated ore source (Degryse et al. 2007). It is important to note, that the slag found in the city dating to the late Roman period is all smithing slag and not smelting slag (Degryse, Schneider, and Muchez 2009). Therefore, it is possible that the origin of the raw material used to produce the subsequent artefacts is outside the city. Although this is still assumed to be somewhere within a relatively close distance to the city (Degryse, Schneider, and Muchez 2009).

Archaeological Interpretations

The results of the qualitative HH-XRF analyses clearly indicate two distinct groups of iron-slag can be indentified in both the laboratory and field samples. The Ti – Zr rich group is predominantly associated with Byzantine material from Dereköy and Tekeli Tepe. Previous research (Degryse, Muchez, Six, et al. 2003) has identified the ore source of this material as being a spinel placer deposit in the Bey Dağlari massif. The samples found in Ağlasun, which group compositionally with the high Ti – Zr group, may have been smelted from the Bey Dağlari ore. The smelting would have occurred close to the ore source and the subsequent material transported to or through Ağlasun for further processing. Further potential groups could also be seen in the qualitative field data in terms of the Mn contents. All of the high Ti samples had high Mn, however, not all of the increased Mn samples had high Ti (Figure 4). The original analysis of the spinel placer deposits did not reveal elevated Mn. Therefore, the ore is not the sole contributor of Mn to these samples. It is probable that Mn is being added to the high Ti – Zr samples as a flux to aid the smelting process. Non-ferrous oxides such as CaO and MnO can substitute for FeO as a flux with SiO_2, thereby freeing up more iron to form a bloom (Iles and Martinón-Torres 2009; Charlton et al. 2010). Since the samples associated with the Bey Dağlari ore do not have elevated Ca contents, it is probable that a Mn-rich flux was used during the smelting of these samples. The low Ti, higher Mn group are mostly survey finds and, as such, have no excavation context and are therefore undated. Likewise, the majority of these slag are undiagnostic. It is possible that the elevated Mn in the low Ti samples either represents the use of a different ore, or the addition of a Mn-rich flux. A Mn-rich ore exists at Camoluk, just outside the territory of Sagalassos (Degryse, Schneider, and Muchez 2009). However, further work is needed to fully characterise this ore, before any definite associations can be made.

There is a potential division between the Ca contents of the samples. This is more apparent when looking at the raw counts rather than the ratios of Ca/Fe. This difference could represent the use of two different ores sources, one richer in Ca than the other. Alternatively, Ca could be being added as a flux. If this is the case, then it suggests that there is more than one iron smelter working in the Sagalassos area. Furthermore, the different iron smelters are using

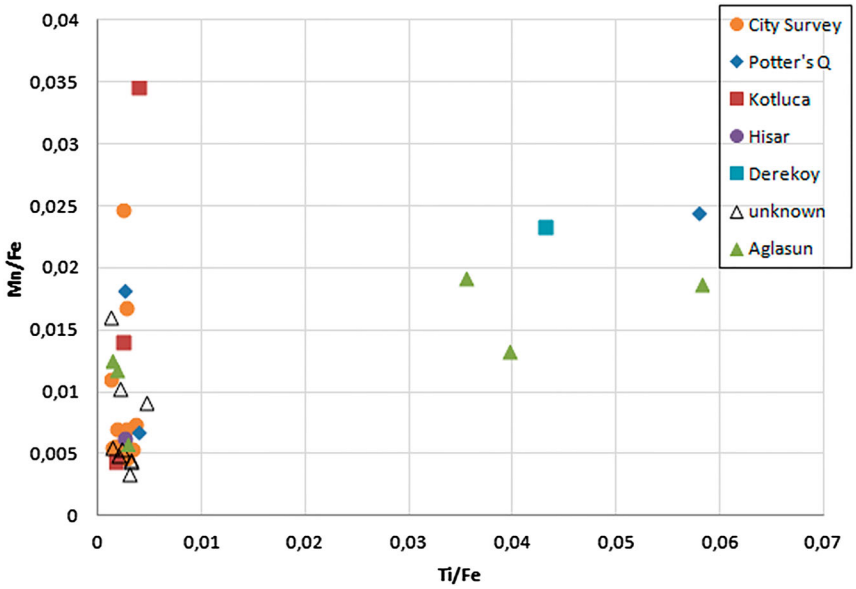

Figure 4 A biplot of Ti/Fe against Mn/Fe showing that all the high Ti samples contain elevated Mn, but not all the elevated Mn samples have high Ti.

different technologies. Most of the slag analysed in this study were non-diagnostic, i.e. the production method could not be identified from a visual field study of the slag remains. However, previous work suggested that the majority of slag found in Sagalassos were smithing slag. Often, silica sand or limestone rich soils could be added to a smithing hearth (Rehder 2000). This enabled the smith to subtly change the composition and subsequent melting point of the slag, making it easier to squeeze out. It is also possible that different smiths in the city were using different fuel sources, which would again alter the Ca content of the slag. A particularly lime-rich fuel source would increase the CaO present in a slag without necessarily indicating the presence of additional flux (Iles and Martinón-Torres 2009). The final composition of the slag can, therefore, be strongly affected by the choice of flux, fuel and furnace conditions (Mameli et al. 2014; van Oss 2002; Degryse, Schneider, and Muchez 2009; Blakelock et al. 2009; Gordon 1997; Iles and Martinón-Torres 2009; Buchwald and Wivel 1998).

Conclusion

As Helmig, Jackwerth, and Hauptmann (1989) concluded the pXRF (or in this case HH-XRF) is extremely useful for screening and grouping the metallurgical samples in the field. The field work at Sagalassos successfully revealed the presence of two groups in the slag, those with a high Ti – Zr signature and those with a low Ti – Zr signature. Based on previous work, this high Ti – Zr group is most probably related to high Ti ores found in the Bey Dagalari region, to the south-east of the city. The smelting operations in this area were also using a Mn-rich flux. This material is also being transported, due to the slag finds from this group in Ağlasun, probably for smithing purposes. Likewise, the low Ti – Zr group associated with elevated Mn, which is mostly found in Sagalassos, was also transported to Ağlasun. This low Ti – Zr group, as yet, has no directly associated ore source. It is possible that the high Mn ore source at Camoluk was exploited, or alternatively, the elevated Mn is again, the result of the flux used.

Although the field data showed two groups, it was necessary to have the laboratory comparison. This is because there was a possibility that different slag could result in a variance in the matrices, which would impact on the HH-XRF measurements. As with any XRF technique a proper understanding of the material prior to analysis is essential in order to ensure that the X-ray physics and resulting data give proper results (Shugar 2009). Powdering was found to be the optimum method of sample preparation for the field. Although powdering does not preserve the structure or phasing present in the slag, the creation of cubes would be impossible in the field. In the context of this study, the powdered samples distinguished the same high Ti – Zr and low Ti – Zr groups in both the field and laboratory data. So, as Helmig, Jackwerth, and Hauptmann (1989) also noted, the variation in the grain sizes between the laboratory and field powdering methods did not affect the final results. However, it was still essential that the grain sizes created in the field were uniform. Ultimately, the success of using a HH-XRF in the field depends on an appropriate research question. While the HH-XRF can be used for classifying samples in the field, it is still recommended that a thorough quantitative laboratory analysis is performed where possible.

Portable XRF technology has improved and miniaturised in the last 25 years; handheld devices are now highly mobile, affordable and easy to operate. Yet, the best method for analysing iron slag in the field remains largely unchanged. It is necessary to analyse matrix

matched material in the laboratory prior to field work in order to determine the optimum operating parameters. These parameters need to be targeted to answer the appropriate research question. In the case of the Sagalassos material two settings were used, 40 kV, 10.9 µA and 9 kV, 20 µA, while these targeted the elements of particular interest for this research, they may not be appropriate for a different project. The best method of sample preparation for iron slag is still powdering; although for a thorough characterisation of the material, samples should be exported to a laboratory and destructively prepared and/or analysed. Successful XRF analysis is still 10% data collection and 90% inspection (Shugar 2009).

Acknowledgements

This research was supported by the Interuniversity Attraction Poles Programme – Belgian Science Policy, Phase VII, 2012–2017, IAP 07/09 CORES. Thanks go to Mike Carremans for assistance with the figures. We would also like to thank the anonymous reviewers for their comments and for improving the manuscript.

References

Blakelock, E., M. Martinón-Torres, H.A. Veldhuijzen, and T. Young. 2009. "Slag Inclusions in Iron Objects and the Quest for Provenance: An Experiment and a Case Studt." *Journal of Archaeological Science* 36: 1745–1757.

Buchwald, V.F., and H. Wivel. 1998. "Slag Analysis as a Method for the Characterisation and Provenancing of Ancient Iron Objects." *Materials Characterization* 40: 73–96.

Carter, T., and M.S. Shackley. 2007. "Sourcing Obsidian from Neolithic Çatalhöyük (Turkey) Using Energy Dispersive X-Ray Fluorescence." *Archaeometry* 49 (3): 437–454.

Charlton, M.F., P. Crew, Th. Rehren, and S.J. Shennan. 2010. "Explaining the Evolution of Ironmaking Recipes - An Example from Northwest Wales." *Journal of Anthropological Archaeology* 29: 352–367.

Craig, N., R.J. Speakman, R.S. Popelka-Filcoff, M.D. Glascock, J.D. Robertson, M.S. Shackley, and M.S. Aldenderfer. 2007. "Comparison of XRF and pXRF for Analysis of Archaeological Obsidian from Southern Peru." *Journal of Archaeological Science* 34: 2012–2024.

Degryse, P., P. Muchez, J. Naud, and M. Waelkens. 2003. "Iron Production at the Roman to Byzantine City of Sagalassos: An Archaeometrical Case Study." In *Archaeometallurgy in Europe Vol. 1*, 133–142. Milan: Associazione Italiana di Metallurgia.

Degryse, P., P. Muchez, S. Six, and M. Waelkens. 2003. "Identification of Ore Extraction and Metal Working in Ancient Times: A Case Study of Sagalassos (SW Turkey)." *Journal of Geochemical Exploration* 77 (1): 65–80.

Degryse, P., J. Poblome, K. Donners, J. Deckers, and M. Waelkens. 2003. "Geoarchaeological Investigations of the 'Potters' Quarter' at Sagalassos, Southwest Turkey." *Geoarchaeology* 18 (2): 255–281.

Degryse, P., J. Schneider, N. Kellens, M. Waelkens, and Ph. Muchez. 2007. "Tracing the Resources of Iron Working at Ancient Sagalassos (South-West Turkey): A Combined Lead and Strontium Isotope Study on Iron Artefacts and Ores." *Archaeometry* 49 (1): 75–86.

Degryse, P., J.C. Schneider, and Ph. Muchez. 2009. "Combined Pb-Sr Isotopic Analysis in Provenancing Late Roman Iron Raw Materials in the Territory of Sagalassos (SW Turkey)." *Archaeological and Anthropological Sciences* 1 (3): 155–159.

Forster, N., P. Grave, N. Vickery, and L. Kealhofer. 2011. "Non-Destructive Analysis Using PXRF: Methodology and Application to Archaeological Ceramics." *X-Ray Spectrometry* 40: 389–398.

Frahm, E. 2013. "Validity of 'off-the-Shelf' Handheld Portable XRF for Sourcing Near Eastern Obsidian Chip Debris." *Journal of Archaeological Science* 40 (2): 1080–1092.

Gordon, R.B. 1997. "Process Deduced From Ironmaking Waste and Artefacts." *Journal of Archaeological Science* 24: 9–18.

Goren, Y., H. Mommsen, and J. Klinger. 2011. "Non-Destructive Provenance Study of Cuneiform Tablets Using Portable X-Ray Fluorescence (pXRF)." *Journal of Archaeological Science* 38: 684–696.

Helmig, D., E. Jackwerth, and A. Hauptmann. 1989. "Archaeometallurgical Fieldwork and the Use of a Portable X-Ray Spectrometer." *Archaeometry* 31 (2): 181–191.

Hunt, A.M.W., and R.J. Speakman. 2015. "Portable XRF Analysis of Archaeological Sediments and Ceramics." *Journal of Archaeological Science* 53: 1–13.

Iles, L., and M. Martinón-Torres. 2009. "Pastoralist Iron Production on the Laikipia Plateau, Kenya: Wider Implications for Archaeometallurgical Studies." *Journal of Archaeological Science* 36: 2314–2326.

Jia, P.W., T. Doelman, C. Chen, H. Zhao, S. Lin, R. Torrence, and M.D. Glascock. 2010. "Moving Sources: A Preliminary Study of Volcanic Glass Artifact Distributions in Northeast China Using pXRF." *Journal of Archaeological Science* 37: 1670–1677.

Kucha, H., M. Waelkens, W. Viaene, and D. Laduron. 1995. "Mineralogy, Geochemistry and Phase Equilibria as Tracers of the Technology or Iron (steel) Making at Sagalassos during the Roman Period." In *Sagalassos III: Report on the 4th Excavation Campaign of 1993*, 273–291. Leuven: Leuven University Press.

Liritzis, I., and N. Zacharias. 2011. "Portable XRF of Archaeological Artifacts: Current Research, Potentials and Limitations." In *X-Ray Fluorescence Spectrometry (XRF) in Geoarchaeology*, edited by M.S. Shackley, 109–142. New York: Springer.

Mameli, P., G. Mongelli, G. Oggiano, and D. Rovina. 2014. "First Finding of Early Medieval Iron Slags in Sardinia (Italy): A Geochemical - Mineralogical Approach to Insights into Ore Provenance and Work Activity." *Archaeometry 56* (3): 406–430.

Mantler, M., and M. Schreiner. 2000. "X-Ray Fluorescence Spectrometry in Art and Archaeology." *X-Ray Spectrometry* 29: 3–17.

Nakai, I., S. Yamada, Y. Terada, Y. Shindo, and T. Utaka. 2005. "Development of a Portable X-Ray Fluorescence Spectrometer Equipped with Two Monochromatic X-Ray Sources and Silicon Drift Detector and Field Analysis of Islamic Glasses at an Excavation Site in Egypt." *X-Ray Spectrometry* 34: 46–51.

Nazaroff, A.J., K.M. Prufer, and B.L. Drake. 2010. "Assessing the Applicability of Portable X-Ray Fluorescence Spectrometry for Obsidian Provenance Research in the Maya Lowlands." *Journal of Archaeological Science* 37: 885–895.

Nicholas, M., and P. Manti. 2014. "Testing the Applicability of Handheld Portable XRF to the Characterisation of Archaeological Copper Alloys." In *ICOM-CC 17th Triennial Conference Preprints, Melbourne*, edited by J. Bridgland, 1–13. Paris: International Council of Museums.

Rehder, J.E. 2000. *The Mastery and Uses of Fire in Antiquity*. London: McGill-Queen's University Press.

Schreiner, M., B. Frühmann, D Jembrih-Simbürger, and R. Linke. 2004. "X-Rays in Art and Archaeology - An Overview." *Advances in X-Ray Analysis* 47: 1–17.

Shackley, M.S. 2010. "Is There Reliability and Validity in Portable X-Ray Fluorescence Spectrometry (pXRF)?" *The SAA Archaeological Record* 10 (5): 17–20.

Shackley, M.S. 2011a. "X-Ray Fluorescence Spectrometry in Twenty-First Century Archaeology." In *X-Ray Fluorescence Spectrometry (XRF) in Geoarchaeology*, edited by M.S. Shackley, 1–6. New York: Springer.

Shackley, M.S. 2011b. "An Introduction to X-Ray Fluorescenec (XRF) Analysis in Archaeology." In *X-Ray Fluorescence Spectrometry (XRF) in Geoarchaeology*, edited by M.S. Shackley, 7–44. New York: Springer.

Shackley, M.S. 2012. "Portable X-Ray Fluorescence Spectrometry(pXRF): The Good, the Bad, and the Ugly." *Archaeology Southwest Magazine 26* (2): 1–8.

Sheppard, P.J., G.J. Irwin, S.C. Lin, and C.P. McCaffrey. 2011. "Characterisation of New Zealand Obsidian Using pXRF." *Journal of Archaeological Science* 38: 45–56.

Shugar, A. 2009. "Peaking Your Interest: An Introductory Explanation of How to Interpret XRF Data." *WAAC Newsletter* 31 (3): 8–10.

Shugar, A.N., and J.L. Mass. 2012. "Introduction." In *Handheld XRF for Art and Archaeology*, edited by A.N. Shugar and J.L. Mass, 17–36. Leuven: Leuven University Press.

Simandl, G.J., R.S. Stone, S. Paradis, R. Fajber, H.M. Reid, and K. Grattan. 2014. "An Assessment of a Handheld X-Ray Fluorescence Instrument for Use in Exploration and Development with an Emphasis on REEs and Related Specialty Metals." *Miner Deposita* 49: 999–1012.

Speakman, R.J., N.C. Little, D. Creel, M.R. Miller, and J.G. Iñañez. 2011. "Sourcing Ceramics with Portable XRF Spectrometers? A

Comparison with INAA Using Mimbres Pottery from the American Southwest." *Journal of Archaeological Science* 38: 3483–3496.

Speakman, R.J., and M.S. Shackley. 2013. "Silo Science and Portable XRF in Archaeology: A Response to Frahm." *Journal of Archaeological Science* 40: 1435–1443.

van Oss, H.G. 2002. "Slag - Iron and Steel." *U.S. Geological Survey Minerals Yearbook*: 70.1–70.6.

Waelkens, M., E. Paulissen, M. Vermoere, P. Degryse, D. Celis, K. Schroyen, B. De Cupere, et al. 1999. "Man and Environment in the Territory of Sagalassos, a Classical City in SW Turkey." *Quaternary Science Reviews* 18: 697–709.